Rebar Corrosion in Mortars Containing Calcareous Filler

O. R. Batic,[‡] J. D. Sota,[‡] J. L. Fernández,[§] B. Del Amo,[†] and R. Romagnoli*,[†]

CIDEPINT-Centro de Investigación y Desarrollo en Tecnología de Pinturas, La Plata, Argentina, LEMIT-Laboratorio de Entrenamiento Multidisciplinario e Investigaciones Tecnológicas, Calle 52 e/121 y 122 (1900), La Plata Argentina, and UNCOMA-Universidad Nacional del COMAHUE, Buenos Aires 1400 (8300), Neuquén, Argentina

Ordinary portland cement can be replaced, partially, by mineral admixtures which modify the properties of concrete and influence rebar corrosion. The most common mineral admixtures are puzzolans, granulated blast furnace slag, calcareous filler, fly ash with high and low lime content, condensed silica fumes, and rice hush ash. There is an increasing tendency to incorporate carbonate additions to mortars. The beneficial effect of calcareous filler addition has been long discussed although not many studies have been made on the effect of this addition on rebar corrosion. In this research, rebar corrosion in mortar containing calcareous filler was studied employing two water/cement (w/c) ratios: 0.50 and 0.65, respectively. It was found that rebar corrosion became important as the w/c increased. The presence of calcium carbonate altered the structure of the passive layer on rebars.

1. Introduction

Rebar corrosion is of great concern because it is probably the most widespread cause of reinforced concrete degradation. Rebar corrosion depends on several factors such as type and surface configuration of rebars, the type of cement employed in the mortar, the dose of concrete, the permeability of concrete, the presence of cracks and fissures, the presence of contaminants and aggressive species (O_2, Cl^-, CO_2, SO_2, S^{2-}, SO_4^{2-}, etc.), the humidity of concrete, the thickness of the concrete layer on rebars, etc.

Mineral admixtures can replace a definite percentage of cement without impairing concrete properties, and sometimes, this replacement may be beneficial. The most common mineral admixtures are puzzolans, granulated blast furnace slag, calcareous filler, fly ash with high or low lime content, condensed silica fumes, and rice hush ash.[1,2]

The incorporation of mineral admixtures does modify the properties of concrete and influences rebar corrosion by modifying the passive layer structure.[1,2] Some of these properties improve due to physical effects derived from the small particle size of these mineral admixtures while others are modified due to cementitious and puzzolanic reactions with these materials. Puzzolanic reactions are the result of the combination of silica from puzzolans and lime produced by the hydration of calcium silicate. This reaction leads to a calcium silicate with lower Ca/Si ratio, fixing free calcium hydroxide. Although similar in nature, the puzzolanic reaction takes place at a lower rate than that corresponding to the hydration of calcium silicate and, as a consequence, it requires an adequate curing process with controlled temperature and humidity conditions. If the adequate curing conditions are not achieved, a more porous mortar would result.[1,2]

The replacement of a cement fraction by mineral admixtures improves concrete properties such as mix proportions, rheological behavior, and hydration of cement. Among other beneficial effects, it must be pointed out that mechanical resistance as well as the resistance to thermal cracking are both increased. Durability of concrete is also improved due to pore refinement and increased adhesion at the paste/aggregate interface, with reduced microcracking.[1−5] Sulfate attack and mortar expansion by alkali-silica reaction diminish as a consequence of free lime immobilization by the pozzolanic reaction. The effect of chloride on rebar corrosion is restrained, at least for lower water/cement (w/c) ratios, because of the chemical reaction and subsequent immobilization of chlorides by cement hydration products.[4−6]

It is important to point out that researchers' opinions about the beneficial effects of mineral admixtures differ from each other.[1−3,7−10] Montemor et al.[7] found that concrete with high fly ash contents carbonates faster because concrete porosity is higher during the first stages of setting, facilitating CO_2 penetration. Andrade and González[8] reported that mineral admixtures may imply some risk for concrete because they react with free lime diminishing alkalinity in the pore solution. However, they recognize that, in most cases, added cements have identical behavior than pure portland cement.

More recently, calcareous filler was employed massively as a mineral admixture with contents ranging from 5 to 35%.[11−13] There are strong arguments about the addition of limestone which lie on both sides of the question.[13,14] The proponents claim significant savings of energy during production without quality degradation and concomitant improvements in some cement and concrete characteristics. It seems that there is an optimal performance value which is achieved when 15−20% of the cement content was replaced by calcium carbonate. Although the filler material has often been considered to be inert, experimental results show that it does influence the hydration processes.[13]

Ingram and co-workers suggested that limestone could replace gypsum because it may react in a similar way with C_3A and due to its effect on cement particle size distribution. However, only 25−50% replacement would be possible without significant and deleterious effects.[15,16]

Neto and Campiteli found that water retention of portland cement slurries did not change with 15% of limestone. In

* To whom correspondence should be addressed. E-mail: roma_roberto@yahoo.com.ar.

[†] CIDEPINT-Centro de Investigación y Desarrollo en Tecnología de Pinturas.

[‡] LEMIT-Laboratorio de Entrenamiento Multidisciplinario e Investigaciones Tecnológicas.

[§] UNCOMA-Universidad Nacional del COMAHUE.

10.1021/ie100045t
Published on Web 07/30/2010

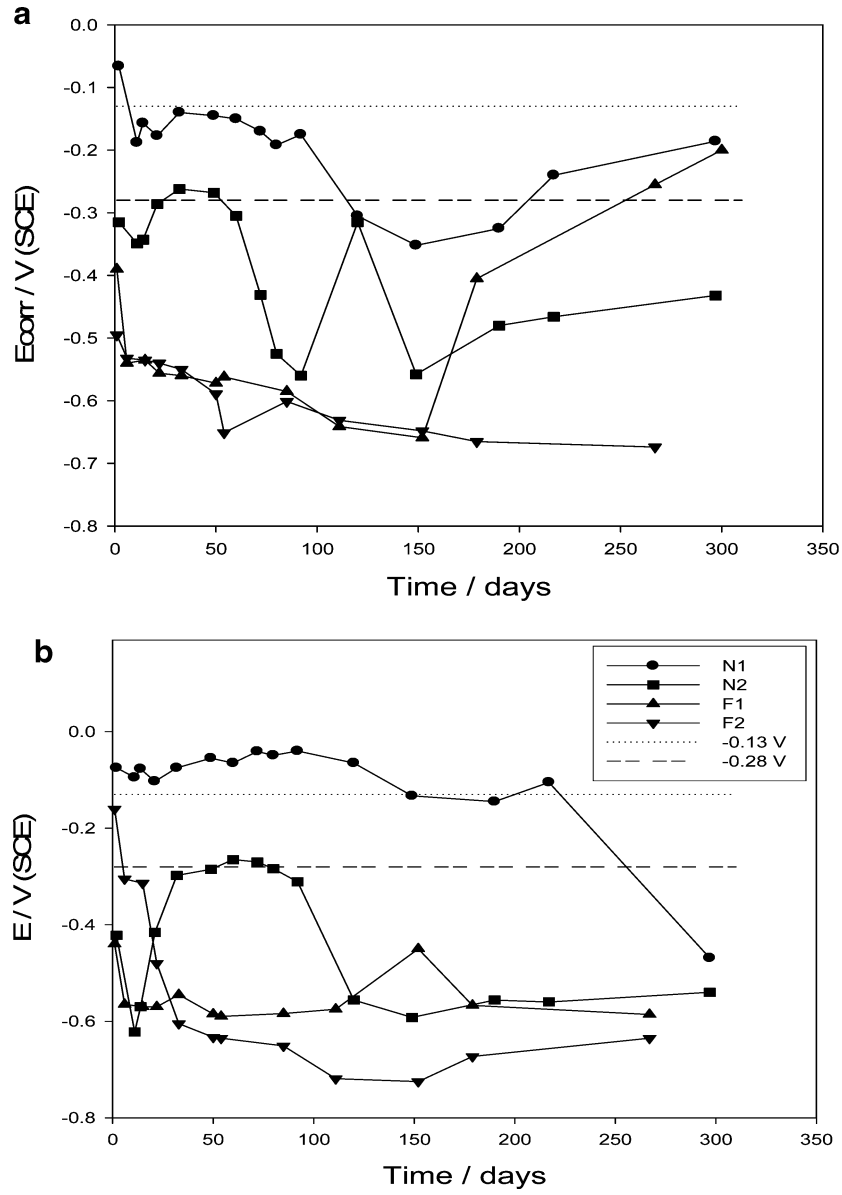

Figure 1. Rebar corrosion potencial as a function of time in different electrolytes: (a) tap water and (b) 3% sodium chloride.

addition, the "lubricity power" of the smaller particles (<10 μm), obtained because of the greater grindability of the limestone, could be appreciated.[17] Carbonate additions have an adverse effect on drying shrinkage of portland cement,[18] but they contributed to accelerate the development of compressive strength and the increase of the curing heat if their content is lower than 15%.[19−21] Carbonate additions do not influence sulfate resistance and the heat of hydration of cements with medium and high C_3A content.[22−26]

Although many investigations have been carried out on the effect of limestone on the hydration of portland cement, little information is available about its influence on rebar corrosion. It was demonstrated that for high filler loadings total porosity increases while bigger pore populations diminish.[11] Chloride permeability seems to be similar to the pure cement when not more than 20% of cement was replaced by calcium carbonate.[21] Tsivilis et al. reported that higher amounts of calcareous filler added to the mortar would result in a more positive corrosion potential.[21]

The objective of this research was to study rebar corrosion in mortars elaborated with portland cement added with calcareous filler and two different w/c ratios (0.50 and 0.65, respectively). The study was conducted in parallel with mortars without the admixture. The behavior of rebars was evaluated by electrochemical techniques: the measurement of corrosion potential and linear polarization tests in tap water and 3% sodium chloride. The nature of the protective layer formed on rebars was observed by scanning electron microscopy (SEM) and its composition obtained by X-ray energy dispersive analysis (EDX).

2. Experimental Section

Cylindrical mortar specimens were cast. A grooved rebar of ordinary hardness (nominally 6 mm diameter, 25 cm long) was inserted along the axis of each specimen. The rebar had a deformation pattern similar to that shown in Figure 1 of ASTM C 234−91a. Its chemical composition was similar to AISI 1040 steel but with a high Mn content (C: 0.40; Mn: 1.00%; Si: 0.40−0.50%; P and Si < 0.02%). The mortar was manufactured with a 1:3 cement/sand ratio by weight and two w/c ratios: 0.50 and 0.65. Ordinary portland cement (OPC, ASTM C 150 Type I), the same cement modified by the addition of calcareous filler, and ordinary graduated siliceous river sand (similar to ASTM

Table 1. Chemical Analysis of Cements Employed in This Research[a]

	loss at (1000 °C)	SiO_2	Fe_2O_3	Al_2O_3	CaO	MgO	Na_2O	K_2O	SO_3	insoluble residue
ordinary portland cement	1.81	23.90	4.35	2.85	62.90	0.59	0.13	0.94	2.10	0.43
cement + carbonate addition	11.63	17.00	2.96	2.83	61.16	0.62	0.12	0.77	2.28	0.63

[a] Results were expressed as % by weight.

C 778) were employed. Calcarerous filler was ground until it had similar particle size distribution to portland cement one, with an average size of ~20 μm. The chemical analysis of the cements employed in this research may be seen in Table 1.

Mortar cylinders (5 × 10 cm in size) were obtained filling the molds in three layers, pressing each layer with a tamper. During the first 24 h, specimens were in the humid chamber (>95% RH and 23 ± 2 °C) and, finally, they were removed from their molds and kept under limewater to complete the 28-day curing period under the same conditions of relative humidity and temperature. Previously to testing, the emerging part of the rebar was coated with an anticorrosive paint formulated with zinc phosphate and chlorinated rubber plus a top coat. The upper and lower surface of the mortar specimens were coated with the same topcoat and sealed with a paraffinic compound. Electrical leads were soldered on the extreme of the emerging rebar. After the curing period, the specimens were immersed in containers filled either with tap water or with a 3% sodium chloride solution, for almost 1 year. The level of the liquid was maintained at 0.5 cm below the upper surface of the mortar specimen.

Electrochemical measurements (corrosion potential and linear polarization) were performed during the test period, in stationary normally aerated solutions. Tests were done in duplicate. The corrosion potential was monitored as a function of time against a saturated calomel electrode (SCE). Linear polarization measurements (with IR compensation) were carried out employing a three electrode cell where the working electrode was the rebar and a SCE and a platinum grid were used as reference and counter electrodes, respectively. The swept amplitude was ±0.150 V from the open circuit potential, and the scan rate was 0.250 mV s^{-1}. Measurements were carried out with a Potentiostat/Galvanostat EG&G PAR Model 273A plus SOFTCORR 352 software. Steel corrosion rates were calculated, from polarization resistance measurements, employing the well-known Stern-Geary equation:

$$\text{Icorr} = B/\text{Rp}$$

where B is a constant whose value is 26 mV for steel in the active state and 52 mV when steel is passivated and Rp is the polarization resistance.[27,28]

Results were interpreted in terms of the values consigned in the document produced by the DURAR project.[29] Once the testing period ended, the rebars were pulled out from the mortars and their surface morphology was studied by SEM employing a PHILLIPS SEM 505 coupled with an EDAX OX PRIME 10 (Energy dispersed form) to determine the surface composition which was expressed as oxide percentages. The EDX device was calibrated with a Zn (30%)−Cu (70%) alloy for both gain and peak position.

3. Results and Discussion

The analysis of the cement employed to carry out this research revealed that it contained 22.32% calcium carbonate, as it may be deduced from the loss on ignition (Table 1). This value is much higher than those recommended by Canadian and American committees.[14] In order to facilitate the analysis of results, each slab was identified with a letter to denote the cement type; N was employed for OPC and F for the cement with calcareous filler. The w/c ratio was named with a number: "1" for w/c ratio 0.50 and "2" for w/c ratio 0.65.

Table 2. Criteria for Predicting Corrosion in Concrete Structures[a]

corrosion potential vs SCE	risk of corrosion	corrosion rate (i/μA cm^{-2})[b]	corrosion level
$E > -0.13$ V	absence of corrosion	<0.1	depreciable
-0.28 V $< E < -0.13$ V	90% probability corrosion is absent	0.1−0.5	moderate
Ecorr < -0.28 V	90% probability of corrosion	0.5−1	high
		>1	very high

[a] SCE: saturated calomel electrode. [b] Data taken from DURAR manual.[28]

3.1. Corrosion Potential. According to the project DURAR,[29] which contain the ASTM C 876 standard specification and is summarized in Table 2, only rebars in mortars with OPC and the lowest w/c ratio exhibited corrosion potentials which indicated the absence of corrosion, in tap water, during the first period of the immersion period (Figure 1a). The rest of the slabs showed more negative values, particularly those with the highest w/c ratio which exhibited values typical of steel undergoing corrosion. The shifting of Ecorr to more negative values could be due to a higher w/c ratio, as in the case of slabs with OPC and w/c ratio of 0.65, or it may be originated by the addition of calcareous filler because the suspension of calcium carbonate has lower pH (~7) than the suspension of OPC.

The tendency for repassivation was observed in both slabs made with OPC and in the specimen with calcareous filler, both with the lowest w/c ratio, at the end of the test period. As a general rule, for specimens stored in tap water, it could be said that the best corrosion behavior was observed in slabs made with OPC and the lowest w/c ratio. The slab with calcareous filler and w/c ratio of 0.50 approached the behavior of the specimen with OPC and w/c ratio of 0.50 at the end of the exposure period due to the passivation process.

As it could be expected, rebar potentials in 3% NaCl were displaced to negative values, from the beginning of the test period, except in the case of specimens containing OPC and w/c ratio of 0.50 (Figure 1b). However, corrosion potential of these specimens evolved to negative values as time went on, and at the end of the test, the rebar surface was corroding. For the highest w/c ratio rebar potential moved, after ~2 months of immersion, from the uncertainty zone to the zone for which the risk of corrosion was 90%. The rest of the test specimens showed potential values corresponding to corroding rebars.

3.2. Corrosion Rate As a Function of Time. Corrosion rates were determined according to the procedures described in the literature, from the measurement of the polarization resistance. The polarization resistance must be regarded as an "apparent polarization resistance because of the presence of transport-limited polarization, uncertainty in the size of the steel surface sampled although the geometric area was known, the presence of a large and non-ideal apparent interfacial capacitance at the steel concrete interface, etc.[28,30] However, Keddam et al. found

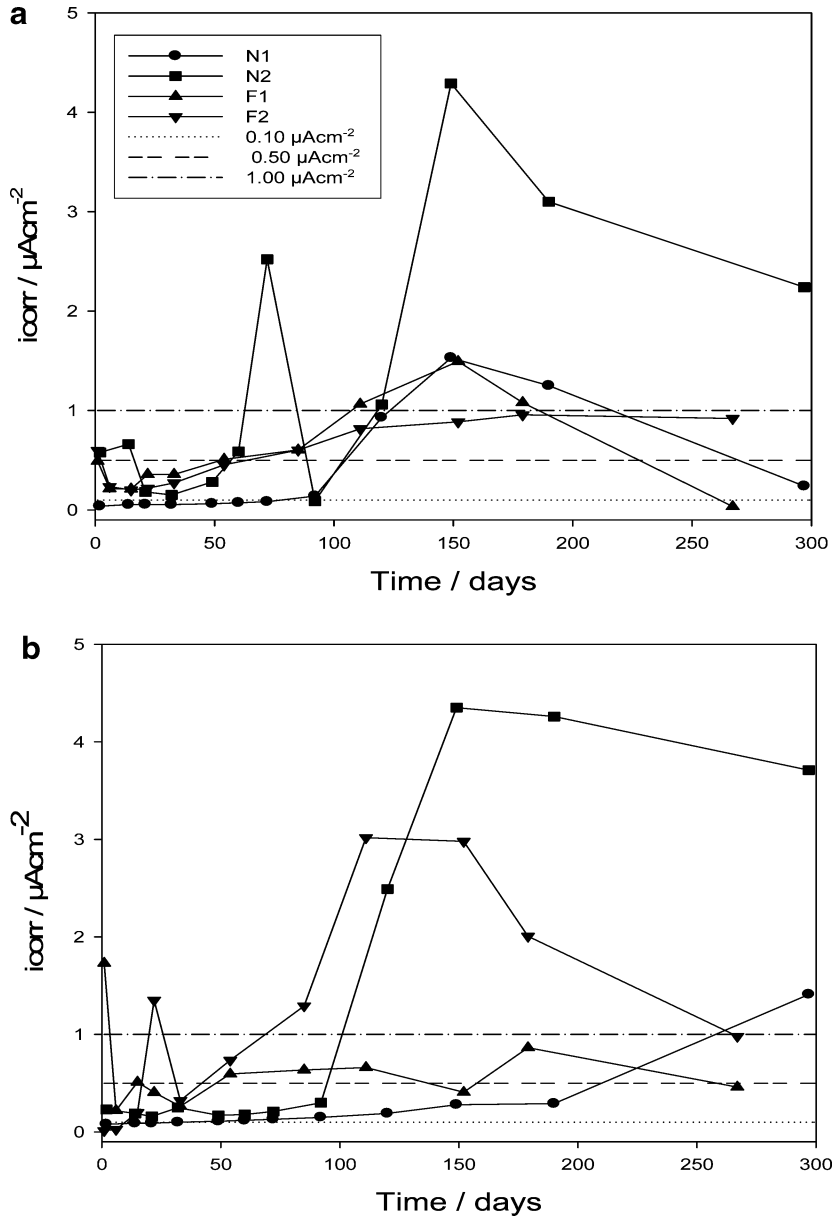

Figure 2. Rebar corrosion rate as a function of time in different electrolytes: (a) tap water and (b) 3% sodium chloride.

a very good correlation between electrochemical impedance measurements and linear polarization measurements.[31]

The analysis of the variation of the corrosion rate as a function of time is of great interest. In tap water, most vales were lower than 0.5 μAcm^{-2} [27] during, approximately, 2 months (Figure 2a). The lowest values were measured for slabs with OPC, and corrosion rate was very low ($\sim$0.10 μAcm^{-2}) for the lowest w/c ratio. However, in some cases, rather high corrosion rates were measured. The abrupt changes in corrosion rate were attributed to changes in the structure of the passive film to finally generate an improved protective layer. The corrosion rate of test specimens containing OPC and F with the lowest w/c ratio was $\sim$1.5 μAcm^{-2} at the end of 5 months of exposure and, then, decreased below 0.3 μAcm^{-2} as time went on. It was supposed that a repassivation process took place because the corrosion rate descended significantly after it. The corrosion rate of slabs with higher w/c ratio were, as expected, higher, but while the corrosion rate of specimens with OPC tended to diminish as time elapsed, the corrosion rate of slabs with calcareous filler increased slightly with time.

In general, none of the specimens immersed in 3% NaCl were in the passive state except slabs N1 and F1 at the beginning of the test which, finally, corroded at a moderate rate as time went on (Figure 2b). The corrosion rate for slabs with w/c ratio of 0.65 was higher and the specimens tended to passivate, but corrosion rates were still high (>1 μAcm^{-2}) after 8 months of exposure.

When OPC was replaced by F, the corrosion rate generally increased. This could be due, in part, to the lower pH of carbonate suspensions ($\sim$7.0). However, F slabs with w/c ratio equal to 0.5 showed a tendency for passivation, evidenced by an oscillating behavior, particularly in tap water. As the w/c ratio increased, the corrosion rate also increased.

3.3. Visual and SEM Analysis of Rebar Corrosion. Once electrochemical tests were finished, rebars were pulled out by lateral compression and observed, in first instance, with the unaided eye. Specimens made with OPC, in tap water, both w/c ratios, only developed small corrosion spots randomly distributed over the entire rebar surface. In change, rebars in 3% NaCl, w/c ratio of 0.65, presented 20−30% of the surface

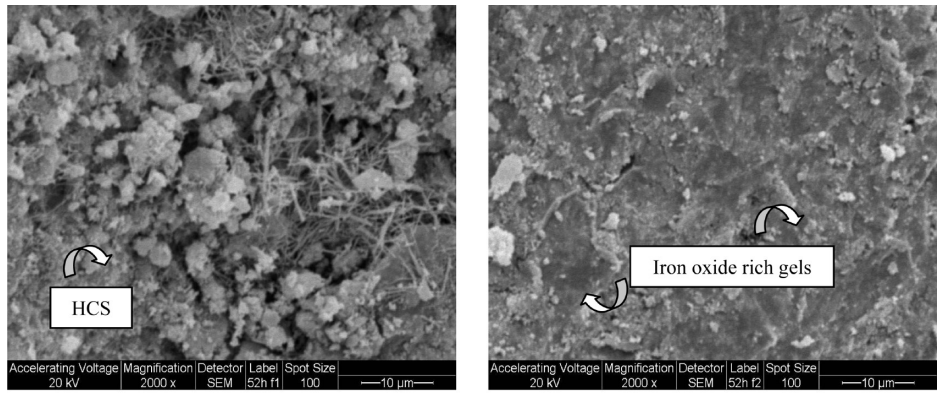

a (2000X) b (2000X)

Figure 3. SEM micrographs of rebars from mortars elaborated with ordinary portland cement. Water/cement ratio: 0.50. Electrolyte: tap water.

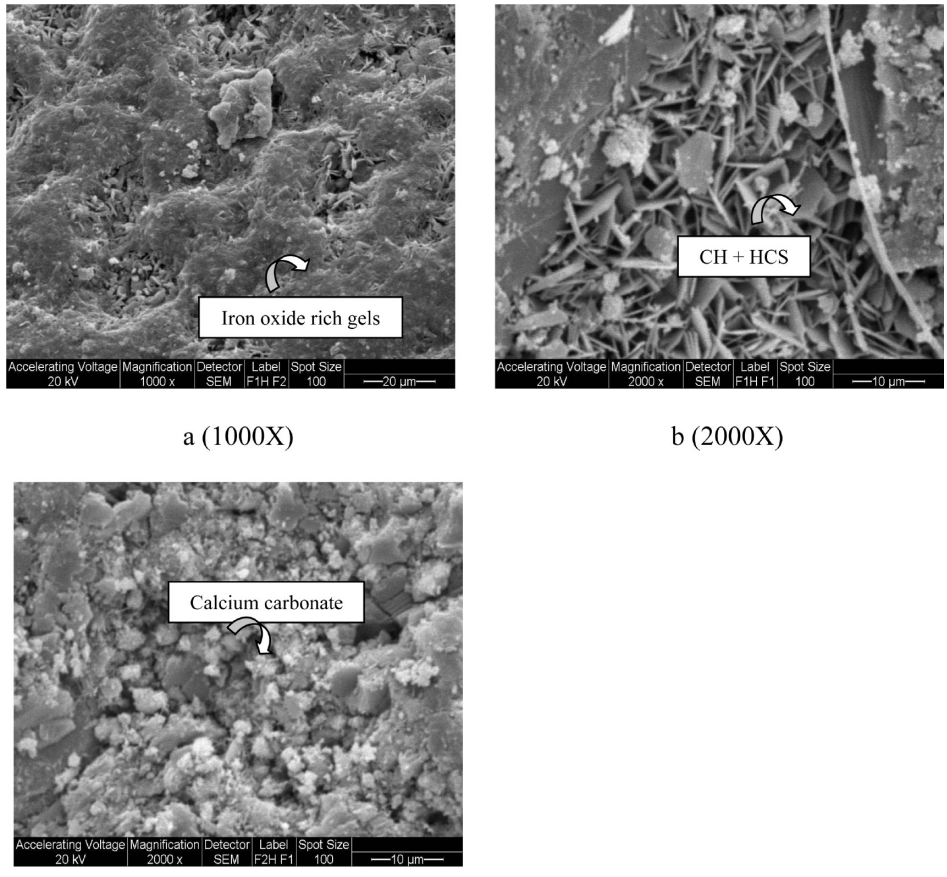

a (1000X) b (2000X)

c

Figure 4. SEM micrographs of rebars from mortars elaborated with portland cement added with calcareous filler. Water/cement ratio of 0.50. Electrolyte: tap water. (a) and (b) structure of the protective layer, (c) film repair in defective areas. CH: calcium hydroxide; HCS: hydrated calcium silicates.

covered with corrosion products. This percentage increased to ~75% when calcareous filler was incorporated to the mortar.

After visual examination, representative samples cut from the rebar were examined by SEM. Cut pieces were obtained in such a way that all formations were present on them; if necessary, several pieces were cut. The presence of carbon dioxide in cut samples was due to calcareous filler because samples were stored in an air tight container from the very moment they were obtained. Results from EDX analysis were expressed as percentage of oxides. One must bear in mind that the surface analysis by the EDAX probe is subjected to a certain error, not higher than 20%, and results must be regarded as semiquantitative. Errors are higher in the case of elements of lower molecular weight. As rebar analysis was comparative, clear tendencies were observed and reported in this section. Iron oxide content in protective rebars was rather high and, sometimes, it may be due to the detection of iron from the substrate because of the low thickness of the protective layer.

Rebars extracted from specimens elaborated with OPC, stored in tap water, presented two well differentiated regions after SEM examination. The most widespread morphology was constituted by gels with filament-like formations (Figure 3a) and was similar to others reported in the literature.[32−36] Spectral data showed that these formations were rich in hydraulic compounds (SiO_2:

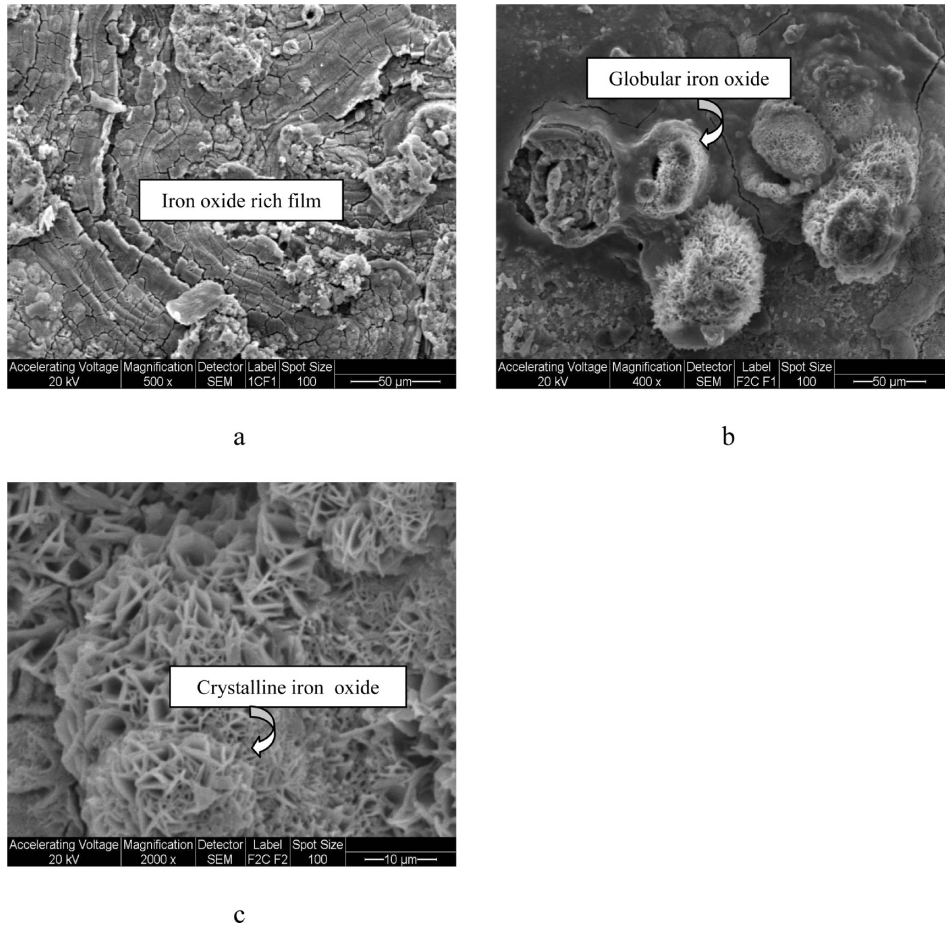

Figure 5. SEM micrographs of rebars from mortars elaborated with portland cement added with calcareous filler. Water/cement ratio: (a) 0.50; (b,c) 0.65. Electrolyte: 3% sodium chloride.

20−25%; CaO: 32−40%) with lower amounts of iron oxides (Fe_2O_3: 11−19%) and carbon dioxide (CO_2: 8−10%). The other morphology contained gels constituted by nonexpansive iron oxihydroxides (Figure 3b). Expansive iron oxides usually exhibit a globular morphology. Although the iron oxide content may be influenced by the base metal, high values (Fe_2O_3: ∼83%) were detected in certain regions of the rebar. When the w/c ratio increased to 0.65, the surface configuration was similar but with a higher amount of these iron oxihydroxides formations.

The surface analysis of rebars pulled from slabs with F, stored in tap water, showed the presence of gel-like formations (Figure 4a) constituted, principally, by iron compounds (Fe_2O_3: ∼57%) and high amounts of carbon dioxide (CO_2: 30−35%). These gels alternated with some differential formations (Figure 4b), rich in calcium oxide (∼28%) and silica (∼9%). These percentages suggested that calcium hydroxide and calcium silicate hydrates were formed. These formations appeared to be carbonated (CO_2: ∼35%) and seemed to be embedded in the iron oxide layer. When the w/c ratio increased, the surface morphology was similar but gels contained a higher amount of iron compounds (Fe_2O_3: ∼67%) and lower amounts of carbon dioxide (CO_2: ∼20%). Apparently, the protective film collapsed in certain regions and was repaired (Figure 4c) by the precipitation of compounds rich in calcium oxide (CaO: 40.4%) and carbon dioxide (CO_2: ∼30%), with the iron oxyhydroxide content being lower (Fe_2O_3: ∼17%). These results lead one to think that calcium carbonate was formed on the passive layer and that the protective layer was constituted by iron oxihydroxides with a high degree of carbonatation which was reduced as the w/c ratio increased, thus imparing the protective ability of the film. Film repair was achieved by precipitation of hydraulic compounds in defective areas.

Rebars in mortars with OPC, submerged in 3% NaCl, were covered by gels and, in certain zones, a fine particulated material deposited on it, as it occurred in tap water with specimens with the lower w/c ratio, both types of cements. The iron content increased as the w/c ratio increased.

The situation is different for the rebar of specimens with F whose surface was covered by a noncontinuous and cracked film (Figure 5a) with a higher iron oxide content (Fe_2O_3: ∼72%) and lower levels of carbon dioxide (CO_2: ∼19%). The presence of chlorides (Cl_2O: ∼3%) was detected in certain regions associated with iron oxides. As the w/c ratio increased, iron compounds with different morphology were formed. Globular formations (Figure 5b), which were intensely carbonated (CO_2: ∼59%), were observed together with crystalline iron oxides (Figure 5c).

4. Conclusions

In general, carbonate additions to OPC impaired mortar protective properties, especially in the presence of chloride, and changed the nature of the protective layer on rebars. Changes in the protective layer are believed to be responsible for changes in the electrochemical behavior. This mineral addition caused rebar to be more susceptible to corrosive attack. The increase in the w/c ratio minimizes the differences between both types of mortars. The role of carbonate additions is to provide carbonate anions to passivate rebars. This passivation process caused corrosion rates not to be so high. Carbonate anions also

deposited on oxide spots which were rendered passive, but this process was not uniform and was of lower intensity in chloride medium.

In spite of the rather high calcareous filler content of the cement studied in this research, it must be concluded that this cement may match the properties of ordinary portland cement if the w/c ratio is low and chloride is absent.

Acknowledgment

The authors are grateful to CONICET (Consejo Nacional de Investigaciones Científicas y Técnicas) CIC (Comisión de Investigaciones Científicas de la Provincia de Buenos Aires) and UNLP (Universidad Nacional de La Plata) for their sponsorship to do this research.

Literature Cited

(1) Kumar Mehta, P. Part II. Concrete materials, mix proportions and early age properties. Admixtures. In *Concrete structures, properties and materials*; Prentice-Hall, Inc.: Upper Saddle River, N.J., 1986; pp 249−285.

(2) Malhotra, W. M. Properties of fresh and hardened concrete incorporating ground, granulated, blast-furnace slag. In *Supplementary cement materials for concrete*; Malhotra, W. M., Ed.; Canadian Government Publishing Center Supply and Services: Ottawa, Canada, 1987; Chapter 5, pp 291−331.

(3) Beaudoin, J. J.; Brown, P. W. The structure of hardened cement paste. Proceedings of the 9th International Congress on the Chemistry of Cement, 1992, 485.

(4) Montemor, M. F.; Simões, A.M. P.; Salta, M. M.; Ferreira, M. G. S. The assessment of the electrochemical behaviour of fly ash containing concrete by impedance spectroscopy. *Corros. Sci.* **1993**, *35* (5−8), 1571.

(5) Montemor, M. F.; Simões, A. M. P. Salta. Effect of fly ash on concrete reinforcement corrosion, studied by EIS. *Cem. Concr. Compos.* **2000**, *22* (2000), 175.

(6) Luo, R.; Cai, Y.; Wang, C.; Huang, X. Study of chloride binding and diffusion in GGBS concrete. *Cem. Concr. Res.* **2003**, *33*, 1.

(7) Montemor, M. F.; Simões, A.M. P.; Salta, M. M.; Ferreira, M. G. S. Carbonatation of fly ash containing concrete: electrochemical studies. In *Electrochemical methods in Corrosion research V−Part 2*; Ferreira, M. G. S., Simões, A. M. P., Eds.; Materials Science Forum, 1995, Vols. 192−194, Part 2, p 867.

(8) Andrade, C.; González, J. A. Técnicas electroquímicas cuali y cuantitativas para medir los efectos de las adiciones sobre la corrosión de las armaduras. *Mater. Constr.* **1981**, *N° 182*, 69.

(9) Bastidas, D. M.; Fernández-Jiménez, A.; Palomo, A.; González, J. A. A study on the passive state stability of steel embedded in activated fly ash mortars. *Corros. Sci.* **2008**, *50*, 1058.

(10) Aperador, W.; Mejía de Gutiérrez, R.; Bastidas, D. M. Steel corrosion behaviour in carbonated alkali-activated slag concrete. *Corros. Sci.* **2008**, *51*, 2027.

(11) Benachour, Y.; Davy, C. A.; Skoczylas, F.; Houari, H. Effect of a high calcite filler addition upon microstructural, mechanical, shrinkage and transport properties of a mortar. *Cem. Concr. Res.* **2008**, *38*, 727.

(12) Kastis, D.; Kakali, G.; Tsivilis, S.; Stamatakis, M. G. Properties and hydration of blended cements with calcareous diatomite. *Cem. Concr. Res.* **2006**, *36*, 1821.

(13) Poppe, A. M.; De Schutter, G. Cement hydration in the presence of high filler contents. *Cem. Concr. Res.* **2005**, *35*, 2290.

(14) Mayfield, L. L. Limestone additions to portland cement. An old controversy revisited. In *Carbonate additions to cement*; Klieger, P., Hooton, R. D., Eds.; ASTM STP 1064: West Conshohocken, PA, 1990; pp 3−13.

(15) Ingram, K.; Poslusny, M.; Daugherty, K.; Rowe, W. Carboaluminate reactions as influenced by limestone additions. In *Carbonate additions to cement*; Klieger, P., Hooton, R. D. Eds.; ASTM STP 1064: West Conshohocken, PA, 1990; pp 14−23.

(16) Campiteli, V. C.; Florindo, M. C. The influence of limestone additions on optimum sulfur trioxide content in portland cements. In *Carbonate additions to cement*; Klieger, P. Hooton, R. D. Eds.; ASTM STP 1064: West Conshohocken, PA, 1990;, pp 30−40.

(17) Neto, C. S.; Campiteli, V. C. The influence of Limestone additions on the reological properties and water retention value of portland cement slurries. In *Carbonate additions to cement*; Klieger, P. Hooton, R. D., Eds.; ASTM STP 1064: West Conshohocken, PA, 1990; pp 24−29.

(18) Adams, L. D.; Race, R. M. Effect of limestone additions upon drying shrinkage of portland cement mortar. In *Carbonate additions to cement*; Klieger, P., Hooton, R. D., Eds.; ASTM STP 1064: West Conshohocken, PA, 1990; pp 41−50.

(19) Bédard, C.; Bergeron, M. The effect of steam curing on high-early strength portland cement containing carbonate addition. In *Carbonate additions to cement*; Klieger, P., Hooton, R. D., Eds.; ASTM STP 1064: West Conshohocken, PA, 1990; pp 55−59.

(20) Nehdi, M.; Mindess, S. Optimization of high strength limestone filler cement Mortars. *Cem. Concr. Res.* **1996**, *26* (6), 883.

(21) Tsivilis, S.; Batis, G.; Chaniotakis, E.; Grigoriadis, Gr.; Theodossis, D. Properties and behavior of limestone cement concrete and mortar. *Cem. Concr. Res.* **2000**, *30*, 1679.

(22) Douglas Hooton, R. Effects of carbonate additions on heat of hydration and sulfate resistance of portland cements. In *Carbonate additions to cement*; Klieger, P., Hooton, R. D., Eds.; ASTM STP 1064: West Conshohocken, PA, 1990; pp 73−81.

(23) Matschei, T.; Lothenbach, B.; Glasser, F. P. Thermodynamic properties of Portland cement hydrates in the system CaO-Al_2O_3-SiO_2-$CaSO_4$-$CaCO_3$-H_2O. *Cem. Concr. Res.* **2007**, *37*, 1379.

(24) Matschei, T.; Lothenbach, B.; Glasser, F. P. The role of calcium carbonate in cement hydration. *Cem. Concr. Res.* **2007**, *37*, 551.

(25) González; Irassar, E. F. Effect of limestone filler on the sulfate resistance of low C_3A portland cement. *Cem. Concr. Res.* **1998**, *28* (11), 1655.

(26) Lothenbach, B.; Le Saout, G.; Gallucci, E.; Scrivener, K. Influence of limestone on the hydration of Portland cements. *Cem. Concr. Res.* **2008**, *38*, 848.

(27) Feliú, V.; González, J. A.; Andrade, C.; Feliz, S. Equivalent circuit for modelling the steel-concrete interface. I. Experimental evidence and theoretical predictions. *Corros. Sci.* **1998**, *40* (6), 975.

(28) Andrade, C.; Alonso, C. Corrosion rate monitoring in the laboratory and on-site. *Constr. Build. Materials* **1996**, *10* (5), 315.

(29) de Rincón, O. T.; de Carruyo, A. R.; Andrade, C.; Helene, P.; Díaz, I., Eds. DURAR. Red Temática XV.B Durabilidad de la Armadura. Manual de Inspección, Evaluación y Diagnóstico de Corrosión en Estructuras de Hormigón Armado. CYTED. Programa Iberoamericano de Ciencia y Tecnología para el Desarrollo. Subprograma XV. Corrosión/Impacto Ambiental sobre Materiales; pp. 133−136.

(30) Sagües, A. A.; Kranc, S. C.; Moreno, E. I. The time-domain of a corroding system with constant phase angle interfacial component: application to steel in concrete. *Corros. Sci.* **1998**, *40* (6), 1097.

(31) Keddam, M.; Nóvoa, X. R.; Soler, L.; Andrade, C.; Takenouti, H. An equivalent electrical circuit macrocell activity in facing electrodes embedded in cement mortar. *Corros. Sci.* **1994**, *36* (7), 1155.

(32) Richardson, I. G. The calcium silicate hydrates. *Cem. Concr. Res.* **2008**, *38*, 137.

(33) Taylor, H. F. W. Nanostructure of C-S-H: current status. *Adv. Cem. Based Mater.* **1993**, *1*, 38.

(34) Chen, J. J.; Thomas, J. J.; Taylor, H. M. Solubility and structure of calcium silicate hydrate. *Cem. Concr. Res.* **2004**, *34*, 1499.

(35) Romagnoli, R.; Batic, R. O.; Vetere, V. F.; Sota, J. D.; Lucchini, I. T.; Carbonari, R. O. The influence of the cement paste microstructure on corrosion and adherence of rebars as a function of the water cement ratio. *Anti-Corros., Methods Mater.* **2002**, *49* (1), 11.

(36) Diamond, S. The microstructure of cement paste in concrete. *8th Int. Congr. Cem. Chem.* **1986**, *4*, 122.

Received for review January 8, 2010
Revised manuscript received June 21, 2010
Accepted July 15, 2010

IE100045T